JCSE The Journal of Corrosion Science and Engineering
ISSN 1466-8858 Volume 18, Preprint 41 submitted 5 August 2015

Effect of Friction Welding Process Parameters on Oxidation and Hot corrosion behaviour of Incoloy 800 H

[1]K.Anand, [2]P. Sreeraj, [1]K.Tamilmannan, [2]S. P. Kumaresh Babu, [3*]P. Sathiya

[1]School of Engineering and Technology, Indira Gandhi National Open University, New Delhi 110016, India.

[2]Department of Metallurgical and Materials Engineering, National Institute of Technology, Tiruchirapalli-620015, Tamilnadu, India.

[3]Department of Production Engineering, National Institute of Technology, Tiruchirapalli-620015, Tamilnadu, India.

*Corresponding author: psathiya @ nitt.edu; Tel.:+91 431 2503510; Fax: +91 431 2500133

Abstract:

High temperature corrosion studies were carried out on friction welded Incoloy 800 H in air and molten salt of Na_2SO_4-60%V_2O_5 at 700^0C under cyclic condition for 50 cycles. Results indicate when heating pressure increase, hot corrosion resistance of the weld decrease. The hot corrosion resistance increases when upsetting pressure increases. Measurement of weight gain or loss were done by Thermogravimetric analysis. It is found that molten salt atmosphere was more corrosion resistance than air oxidation atmosphere. The oxide scales formed on weldment were analysed by XRD, SEM/EDS. The influence of welding parameters on hot corrosion under different environments were discussed in this paper.

Keywords: Incoloy 800 H, Friction welding, hot corrosion, XRD, SEM&EDS.

1. Introduction

Incoloy 800 H alloy is commonly used above 600^0C where resistance to creep and rupture is the prime requirement. Incoloy 800 H is a Fe-Ni superalloy used in a variety of applications involving exposure to corrosive environments and high temperatures such as heat treating equipment, chemical and petrochemical processing industry, nuclear power plants and paper pulp industry [1-3]. Heat treating equipments such as baskets, trays, fixtures employ Incoloy 800 H and chemical and petrochemical industry use incoloy 800 H in heat exchangers and piping system in nitric acid media especially where resistance to chloride stress corrosion cracking required. Incoloy 800 H will not become brittle even after a long period of usage in

ISSN 1466-8858 Volume 18, Preprint 41 submitted 5 August 2015

the 600 ^{0}C-900 ^{0}C range where many stainless steels become brittle. Incoloy 800 H can welded by common techniques used on stainless steels. Friction welding is a solid state joining process and it is the most economical and also feasible method in joining similar and dissimilar metals [4]. It is used extensively due to the advantages such as low heat input, production efficiency, ease of manufacture and environment cleanliness. Friction welding does not involve melting and solidification and so it gives uniform weld bead without any microsegregation within the dendritic structures which give less corrosion susceptibility [5-6].

The major problem encountered in dissimilar welding of Incoloy 800 H and stainless steel is the formation of brittle intermetallics at weld interface which reduces corrosion resistance of weld joint [7]. In hot corrosion, molten salt(s) forms a film on a metal surface that fluxes and destroys the normal protective oxide layer [8-10]. In fossil fuel, during combustion impurities like Na, V and S melt or vaporise and get deposited on metal parts. Combustion product involves Na_2SO_4 which attacks the metals protective layer and undergo fluxing and metal consumption [11]. Vanadium the impurity from fuel oil, forms V_2O_5 having melting point 670 ^{0}C that produces serious corrosion [12]. The problem gets compounded by the formation of V-Na mixed oxides having melting point at 545 ^{0}C. It was reported that Incoloy 800 H showed better oxidation resistance than Incoloy 825 when both exposed to 1000 ^{0}C and 1200 ^{0}C [13-16]. Tan et al. [17] conducted the grain boundary examination (GBE) on Incoloy 800 H employed in supercritical water to evaluate the air oxidation behaviour at 550° C. It was found that GBE resulted in the spallation resistance of the Incoloy 800H and also reduced the corrosion rate. Dehmolaeib et al. [18] studied the microstructure and mechanical properties of Incoloy 800 H after exposing it to 15 years of use. It was observed, the improvement in hardness and strength and decrease in ductility and toughness were due to the formation of primary carbides and secondary precipitates after a long time exposure.

A review of the available literature, clearly indicates that only a very limited work was carried out on hot corrosion studies on welding of Incoloy 800 H joints. So far no visible work has been focused on friction welding of Incoloy 800 H joints particularly under Na_2SO_4 - V_2O_5 environments.

The main objective of this work is to study the hot corrosion behaviour of friction welding of Incoloy 800 H in molten salt of Na_2SO_4-60%V_2O_5 and air oxidation under cyclic conditions at 700 ^{0}C. And also to find the effects of welding parameters on hot corrosion resistance of the

ISSN 1466-8858 Volume 18, Preprint 41 submitted 5 August 2015

weldments. Thermogravimetric technique was used to plot corrosion studies. The hot corroded weldments were further analysed by XRD, SEM and EDAX.

2. Experimental Procedure

2.1 Friction welding

Friction welding was done by a 150-kN continuous drive friction welding machine. Friction welding parameters were fixed based on the optimized results [19]. The optimized friction welding parameters are shown in Table 1. The friction welded specimens are shown in Figure 1.

Table. 1 Welding parameters

Exp. No	Heating pressure (Mpa)	Heating time (sec)	Upsetting pressure (Mpa)	Upsetting time (sec)
Sample 1	60	8	180	6
Sample 2	105	**7**	180	8
Sample 3	75	5	150	6

Figure 1. Friction welded samples

Base material chemical composition is presented in Table 2.

Table 1 Base material chemical composition (wt.%)

C	Si	Mn	Cr	Mo	Ni	Al	Cu	Nb	Ti	Fe
0.06	0.29	0.93	20.14	0.08	30.28	0.58	0.18	0.03	0.56	45.1

2.2 Macrostructure and Microstructure

The weld samples were cut in to the required size (10X10 mm) and the samples were prepared as per the Metallographic standards. The joint regions were polished by emery sheets of SiC with grit size varying from 220 to 1000 µm and then subjected to disc polishing using alumina to obtain mirror polish up to 1µ. Then electrolytic etching (10% oxalic acid

ISSN 1466-8858 Volume 18, Preprint 41 submitted 5 August 2015

solution, 6 V DC supply and 1 A/Cm^2) was used to examine the macro and microstructure of the joint interface.

2.3 Hot corrosion test

The samples were cut into dimensions of 20X7X2 mm by wire cut EDM for conducting the hot corrosion studies. The weld zone was located in the mid span of the specimen. Mirror polished specimens were coated with salt Na_2SO_4-60%V_2O_5 uniformly over the surface with 3-5 mg/cm^2 by a hair line brush on the calculated surface area of the specimen. The samples were kept in ceramic boats and preheated up to 250^{0}C in tubular furnace to eliminate moisture content in salt and weighed for initial mass along with boats. Then they were placed in the furnace at 700^{0}C. After each cycle, weight changes were measured along with boat by electronic weighing balance having sensitivity up to 1 mg. Each cycle had 1 hr heating and 20 min cooling. This was undergone up to 50 cycles. Thermogravimetric plots were created based on the results. The samples after corrosion test were subjected to SEM /EDS, XRD.

3.0 Results

3.1 Macrostructure and Microstructure of the weld joints

The typical macrograph of the friction joint is shown in Figure 2. It is observed that the joint interface is clearly visible and particles are also evenly distributed on the both side of the joint interface.

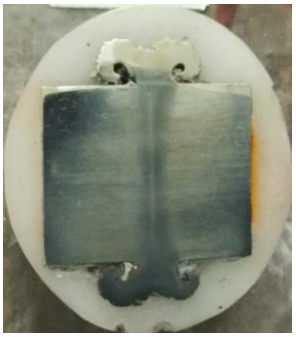

Figure 2 Typical Macrograph of the friction joint

The microstructure of the base metal and weld metal with different welding parameters are shown in Figure 3 (a-d). From Figure 3 (a), well defined grain boundaries and fully austenitic matrix are observed. Cubic precipitates are also found to be present along the grain boundaries. It may be due to the presence of titanium and nitrogen, and it may lead to form nitride or carbonitride of titanium. The spherical precipitates are rich in titanium and carbon

ISSN 1466-8858 Volume 18, Preprint 41 submitted 5 August 2015

and may be identified as titanium carbide (TiC). And additionally annealing twins are also observed in the base metal.

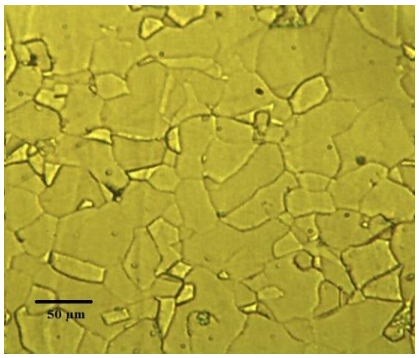

(a) Base material

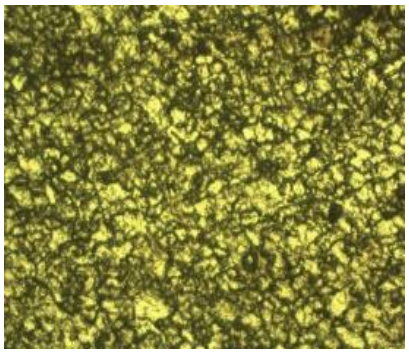

(b) weldmetal-Sample 1

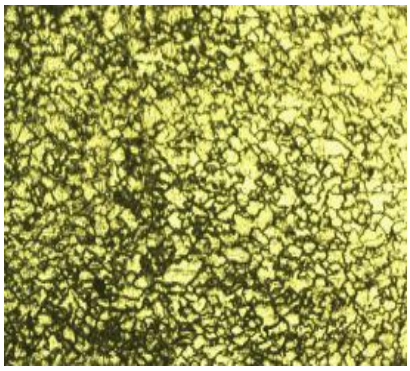

(c) weldmetal- Sample 2

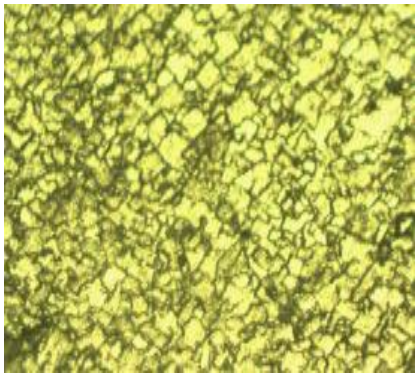

(d) weldmetal - Sample 3

Figure 3 (a-d). Friction weld microstructure of Incoloy 800 H

Figure 3 (c) revels a very fine grain size in the weld metal microstructure. This is due to higher upsetting pressure. When friction components undergo the high upsetting pressure, the metal particles are crushed (rubbing action) and they become finer. In comparison to base material microstructure, all three friction weld microstructures obtained are of fine grain size with well indentified grain boundaries. The weld metal microstructures are homogenous with particles precipitated along the grain boundary. All weld metal joint interface microstructure mainly consisted of austenite phase. The weld joint interface grains are mainly elongated structure with a very few equiaxed grains.

3.2 Thermogravimetric analysis of Friction weldments of Incoloy 800 H

Thermogravimetric plots are constructed for molten salt environment and air oxidation environment as shown in Figure 4 and Figure 5 respectively. The x-axis is a function of time (number of cycles) and y-axis is a function of weight changes per unit surface area (mg/cm^2). It is observed from Figure 4, that when number of cycles increases, weight gain per surface

ISSN 1466-8858 Volume 18, Preprint 41 submitted 5 August 2015

area is also increases. The uniform weight gain obtained in each and every two cycles is increased. This may be due to uniform corrosion rate happening in all the weld samples.

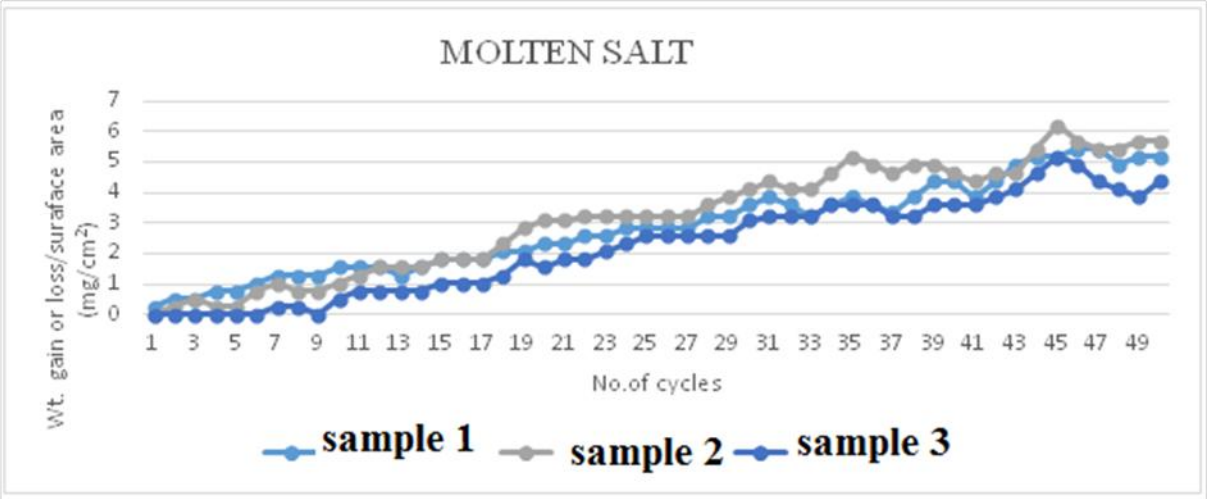

Figure 4. Weight change (mg/cm^2) in cyclic air oxidation with respect to exposed time (hr)

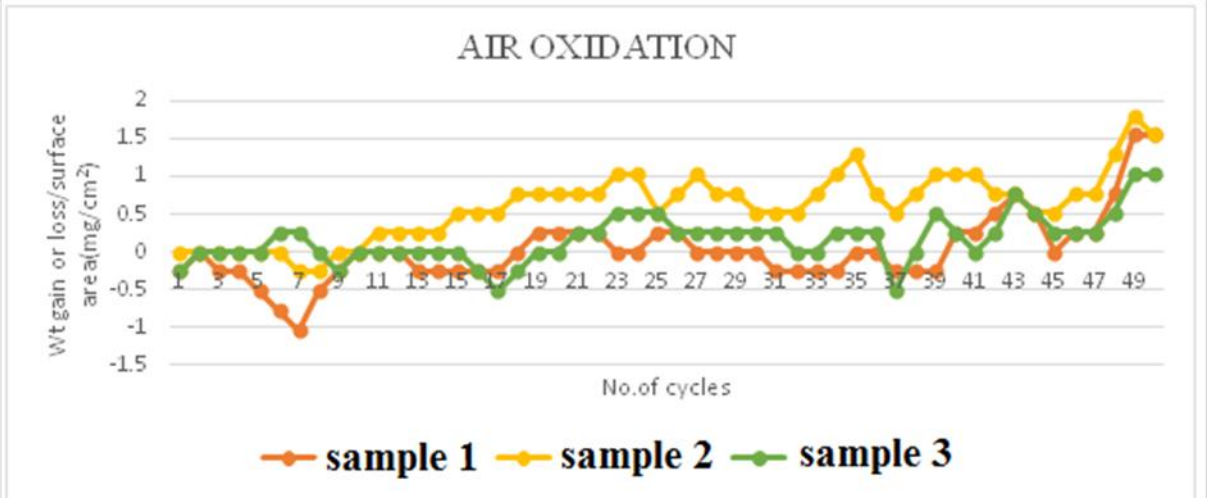

Figure 5. Weight change (mg/cm^2) in cyclic hot corrosion with respect to exposed time (hr)

3.3 XRD Studies

The XRD analysis of the corroded samples of Incoloy 800 H is conducted. The images of the six samples are shown on Figure 6. From the XRD it is identified that the scales containing CrO_2, CrO_3, TiO_2, Al_2O_3 are commonly seen in all samples both in air oxidation and molten salt environment. All samples in molten salt environment contain an additional $NiCr_2O_4$ and Fe_3O_4 oxide scale. Samples in air oxidation contain an additonal oxide scale of NiO. Out of

JCSE The Journal of Corrosion Science and Engineering
ISSN 1466-8858 Volume 18, Preprint 41 submitted 5 August 2015

all three hot corroted samples, in air oxidation the first sample set of weld contains Fe_3O_4 oxide in the scale and in molten salt environment it contains additional MnO oxide.

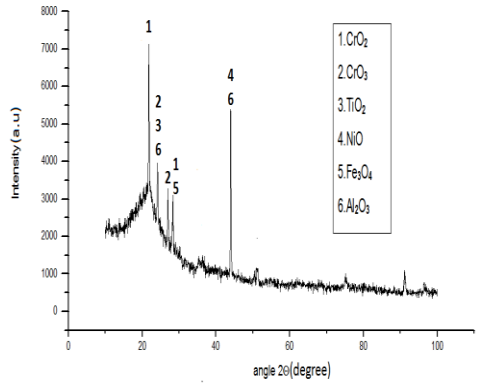

(a)Sample 1 air oxidation

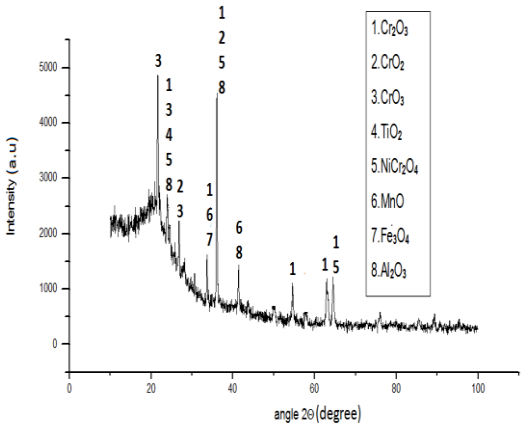

(b) sample 1 in molten salt

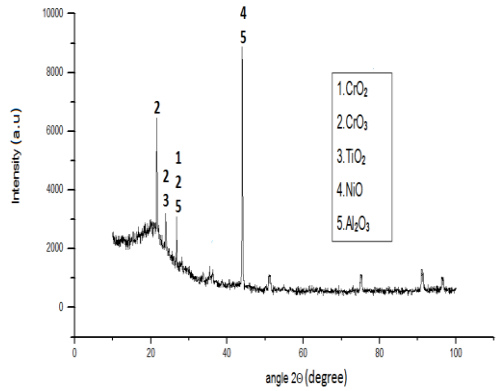

(c) Sample 2 air oxidation

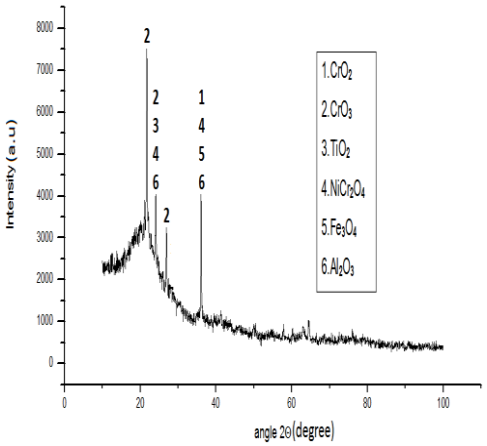

(d) sample 2 in molten salt

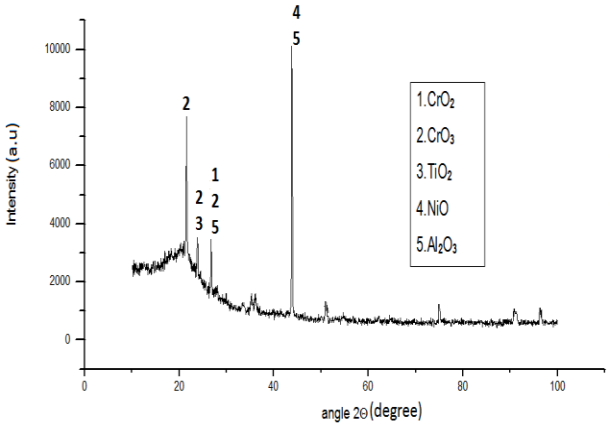

(e) Sample 3 air oxidation

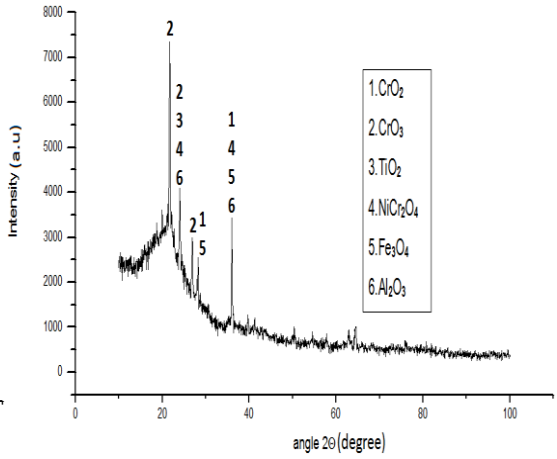

(f) sample 3 in molten salt

Figure 6 (a-f) XRD diffraction plots for hot corroded friction welds under different environments

JCSE The Journal of Corrosion Science and Engineering
ISSN 1466-8858 Volume 18, Preprint 41 submitted 5 August 2015

From Figure 6 (a-f), it is observed that CrO_2, CrO_3, $NiCr_2O_4$, Al_2O_3 have been predominated with lower intensities of TiO_2, NiO and Fe_3O_4. Higher amount of CrO_2, CrO_3, $NiCr_2O_4$, Al_2O_3 are present in molten salt environments compared to air oxidation at 700^0C.

3.4 SEM/EDS analysis

SEM images of hot corroded samples along with elemental energy dispersive spectroscopy (EDS) analysis are shown in Figure 6 (a-g). Here strong and weak peaks of EDS spectrum reveal the presence of elements diffused from substrate to upper most part of scale during hot corrosion. Globular and needle like features mainly associated with iron and chromium oxides are observed in all the samples Figure 6 (a-g). No sulfidation attack is observed on the top scale of all samples. But the flaky and cuboids shaped structures are mainly associated with iron and chromium oxides with little amount of nickel. The presence of titanium oxides are seen in sufficient quanitity.

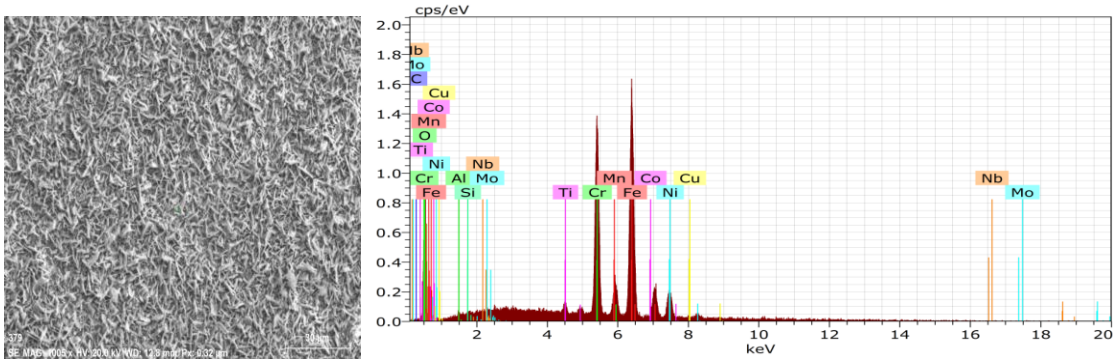

(a) base metal under molten salt

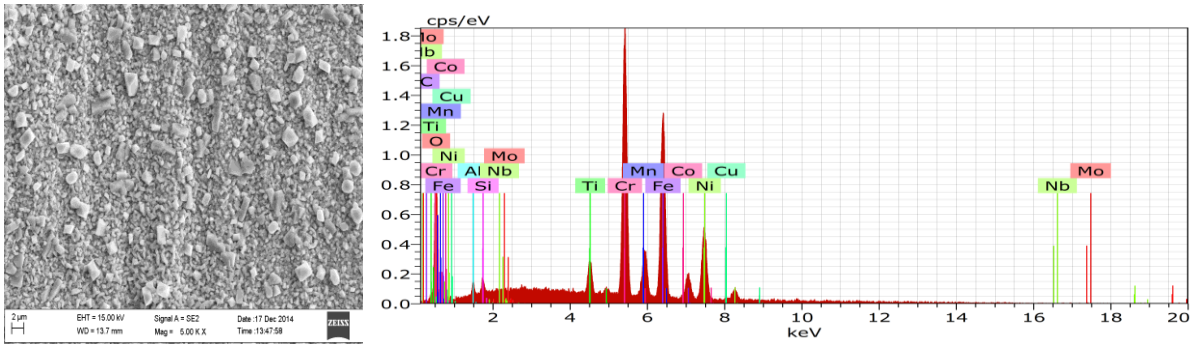

(b) sample 1 weldment under air oxidation

JCSE The Journal of Corrosion Science and Engineering
ISSN 1466-8858 Volume 18, Preprint 41 submitted 5 August 2015

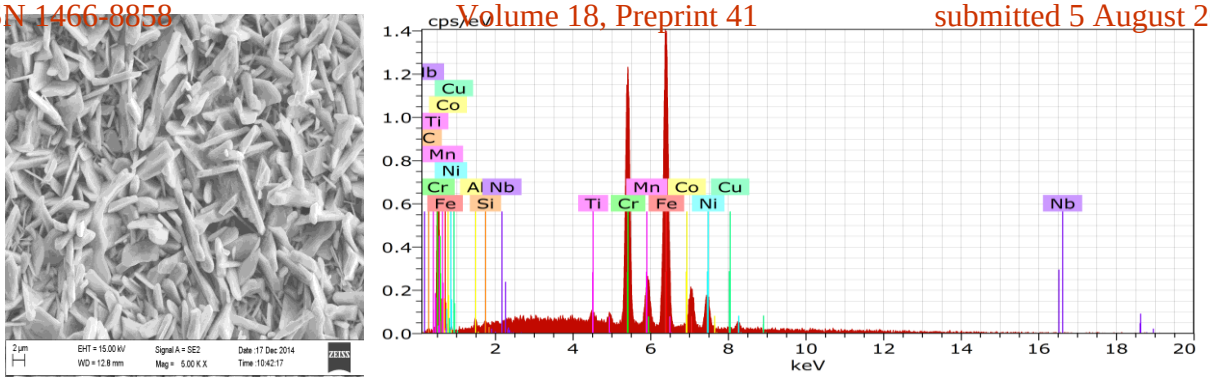

(c) sample 1 weldment under molten salt

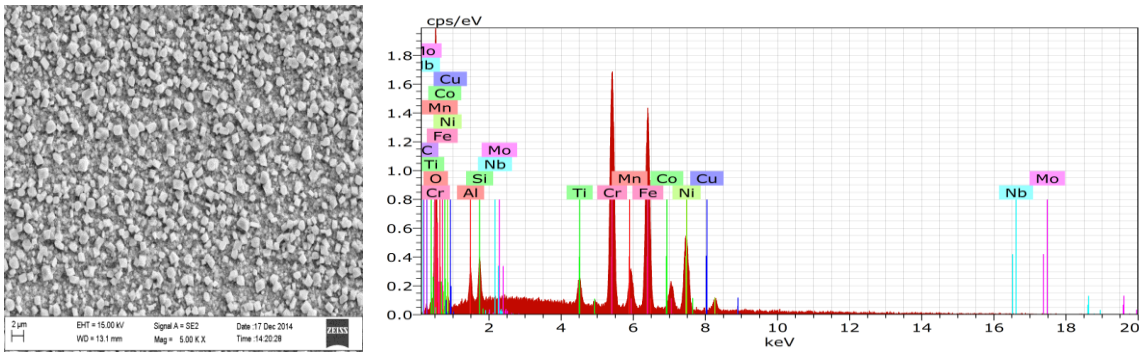

(d) sample 2 weldment under air oxidation

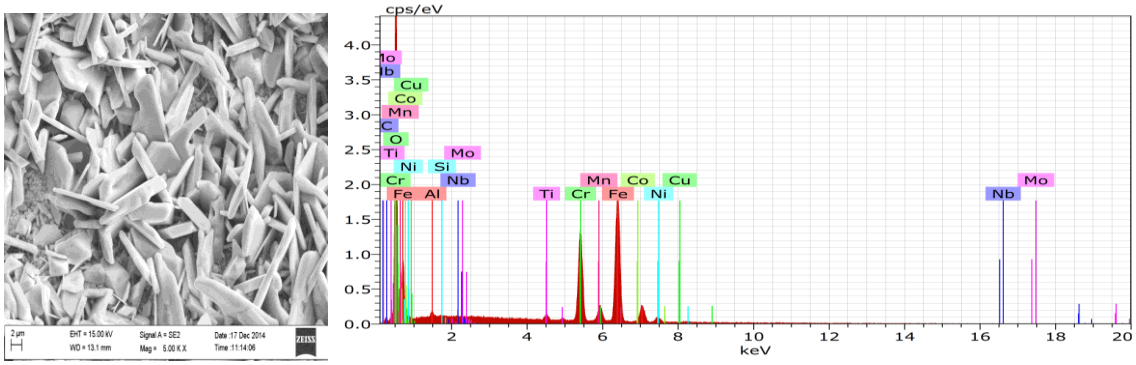

(e) sample 2 under molten salt

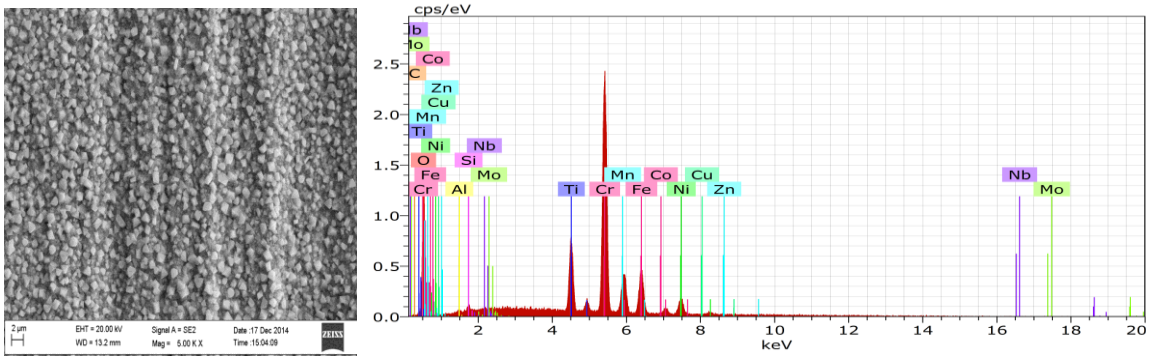

(f) sample 3 under air oxidation

ISSN 1466-8858 Volume 18, Preprint 41 submitted 5 August 2015

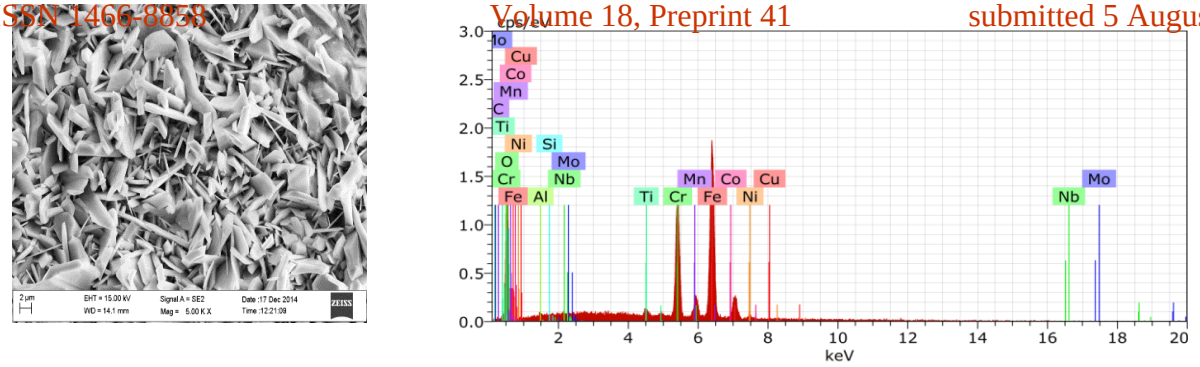

(g) sample 3 under molten salt environment

Figure 6 (a-g) SEM images & EDS plots of weld samples under different environments

4. Discussions

The results obtained in air oxidation at 700°C (Figure 4 & 5) have been a better corrosion resistance as compared to molten salt environment. The weight change observed in air oxidation is less compared to mixed salt environment. Slight change in weight is observed in air oxidation while a gradual increase is observed in mixed salt. This is due to the molten deposit on the metal surface at high temperature which causes the formation of passive oxide layers and diffusion of oxygen through fused salt to metal surface. Initially chromium ions are transported over the surface of sample to form chromia scale. After some cycles the additional chromium ions get diffused through depleted layer to meet oxide-metal boundary. Thermogravimetric curve of molten salt environment studies shows the tendency of multi stage weight-gain growth rate to be uniform at regular intervals. It could be due to changes in reaction rate which are associated with the formation of a laminated inner-oxide layer made up of fine and coarse grain spinal oxide as suggested by Hurdus et al [11]. In a molten salt environment, sulfur was incorporated into scale and leads to a sulfide formation in the alloy substrate. Therefore, as the formation of protective oxide scale was inhibited by the presence of NaCl, chlorides and sulfides tend to form in the alloy substrate as indicated leading to the propagation of hot corrosion as suggested by Charng et al., [12]. When thermogravimetric plots are analysed it is found that sample welded with higher heating pressure has lower corrosion resistance under condition that upsetting pressure remain same. Hence when upsetting pressure increased, the corrosion resistance will also increase even though the sample has higher heating pressure. From this it is understood that upsetting pressure has higher influence than the friction pressure when corrosion resistance is considered. The presence of oxides like CrO_2, CrO_3, Cr_2O_3, NiO, $NiCr_2O_4$, Al_2O_3, and TiO_2 are identified from XRD analysis. In hot corrosion studies no trace of FeO is found because when Cr

ISSN 1466-8858 Volume 18, Preprint 41 submitted 5 August 2015

content increases it suppresses the formation of FeO. The formation of Chromium oxides, NiO, $NiCr_2O_4$ will protect the surface. But as corrosion time increases the rapid cyclic heating and cooling of metal may cause thermal shock and affect the protective oxide layer to cracking and spallation. The presence of Ti, Mn, and Al in the weld zone also forms protective layer in addition to regular oxide which will increase corrosion resistance to the weld zones.

5. Conclusions

On the basis of this investigation, the following conclusions can be drawn.

- From thermogravimetric analysis, it is seen that molten salt atmosphere had more corrosion resistance than air oxidation atmosphere.
- Hot corrosion resistance of the weld decreases when heating pressure increases.
- Hot corrosion resistance of the weld will increase when upsetting pressure increases. It is understood that upsetting pressure has higher influence than friction pressure when corrosion resistance is considered
- At higher upsetting pressure, the weld metal microstructure has very finer grains.

6. References

(1) David, J.R., (2000) Nickel, cobalt, and their alloys. ASM Specialty Handbook. ASM International.

(2) Donachie, M.J., Donachie, S.J., (2002) Superalloys a technical guide. 2nd ed. United States of America: ASM International.

(3) Daris, J.R., (1999) Metallurgical processing and properties of superalloys. ASM handbooks, vol. 16, No. 18, pp.16-23.

(4) John Figert, Dan Rybicki: NASA M&P UPDATE (NMPU), NASA M&P (1998), Newsletter.

(5) Arivazhagan, N., Surendra, S., Prakash, S., and Reddy, G.M., (2011), *Mater. Des.*, vol. 32, pp 3036.

ISSN 1466-8858 Volume 18, Preprint 41 submitted 5 August 2015

(6) Ozdemir, N.A., Sarslmaz, F., and Hascalk, A., (2007), *Mater. Des.*, vol. 28, No. 1, pp. 301.

(7). Stringer, J., (1977), Hot Corrosion, Annual Reviews Material Science, vol. **7**, pp. 477.

(8). Rapp, R.A., (1986), Chemistry and Electrochemistry of Hot Corrosion of Metals, Corrosion, vol. **42**, pp. 568.

(9). Brnstein, N.S., DesGrescenti, M.A., (1971), Met. Trans., vol. **2**, pp. 2875.

(10). Malik, A.U., et.al, (1989), Materials Trans., JIM, vol. **30**, pp. 7071.

(11). Swisher, J.H. and Shankarnarayan, S., (1994), Inhibiting Vanadium Induced Corrosion, Materials Performance, vol. **33, No.** 9, pp. 49.

(12) Khalid, F.A., Hussain, N., Shahid, K.A., (1999), Microstructure and morphology of high temperature oxidation in superalloys. Materials Science and Engineering A, vol. 265, pp. 87–94.

(13) Raja Gautam, Santhosh, T., Vasantha Kumar, Sunanth Anand, Arivazhagan, N, Devendranath Ramkumar, K. (2013), Comparative Studies on Incoloy 800 H weldments exposed to air oxidation at 600 °C, Journal of Corrosion Science and Engineering, vol. 16, pp. 1-7.

(14) Bhanu Sankara Rao, K., (1994), On massive carbide precipitation during high temperauture low cycle fatigue in alloy 800H, Scripta Met., Vol 31, No 4, pp. 381-386.

(15) Viktor Guttmann and Jens Timm, (1990), On the influence of the thermal pre-treatment on creep and microstructure of alloy 800H, Z Metallkd, vol. 81, No. 6, pp.428-432.

(16) Todd, J.A., and Ren, J., (1989), The effect of cold work on the precipitation kinetics of an advanced austenitic steel, Mater. Sci. Eng. A, vol. 117, pp. 235-245.

ISSN 1466-8858 Volume 18, Preprint 41 submitted 5 August 2015

(17) Yan L., Sridharan, K., Allen, T.R., (2006), The effect of grain boundary engineering on the oxidation behavior of INCOLOY alloy 800H in supercritical water. Journal of Nuclear Materials, vol. 348, pp. 263–271.

(18) Dehmolaeib, R., Shamaniana, M., Kermanpura, K., (2009), Microstructural changes and mechanical properties of Incoloy 800 after 15 years service, materials characterization, vol. 6 0, pp. 246 – 250.

(19) Anand, K., Birendra Kumar Barik, Tamilmannan. K., Sathiya, P., (2015), Artificial neural network modeling studies to predict the friction welding process parameters of Incoloy 800H joints, Engineering Science and Technology, an International Journal, vol. 18, pp. 394-407.